VARIATION OF DRIVING CONCENTRATION WITH DRIVER PERCEPTION THROUGH IN-CAR VIEW ROAD SCENE AS VISUAL STIMULANT

Sevcan AYTAÇ KORKMAZ

Fırat University, Department of Electronic Technology, Elazığ- TURKEY

sevcanaytackorkmaz@gmail.com

Abstract: To make driver generate a right decision as evaluating scenes perceiving by his brain, several factors (objects with different shapes, movements, and illuminations) that effects on driving concentration are existed. In this study, continuously changing scenes that are seen by driver eyes through windshield are statistically investigated. Here I have initially extracted a set of features. Then I have found optimal feature subset using Linear discriminant analysis. And then I get a measure to indicate driver concentration using Jensen Shannon Inequality and Hellinger distance. It has been validated the measures via relationships between them. Consequently, a model is proposed for seeking how the scene influencing on driver concentration as an effective factor for comfortable driving. It suggests concentration risk rate of *fr* is less than all the other road models. However, concentration risk rate of *rsfs* is more than all the other road models.

Keywords: Vehicle environment perception, Jensen Shannon Divergence and Hellinger measure, feature selection, Linear discriminant analysis

Introduction

Motivation

There are many factors that influence on driver performance such as car interior design, suspension, technical specifications, road conditions, traffic density, changing climatic conditions, behavior of other vehicles, vehicle accessories in the placement. A very important factor that influences on driving comfort is also the scene through the windshield. In many studies conducted so far, one or a few factors have been taken into account. However, scene through windshield plays an important role in driver psychology, which has not been intensively investigated. As a matter of this fact in many trading areas I prefer background decoration with different colors considering customer mood. For instance, blue colors are used in a fishery shop; dresses with white, green or blue colors are preferred in hospital; relaxing wall paintings are chosen in resorts, and different decorations are used to increase working efficiency. Hence, depending on landscape in our environment I can sense specified perceptions in our brain. Therefore, I can come up with different ideas via this hypothesis for vehicle drivers who face with many visual landscapes on steering wheel. Different lights, colors, patterns and geometries of the landscape have positive or negative effect on driving performance. Drivers can be aggressive when they look through specified landscapes although some of scenes can improve his driving performance.

Problem Statement

There are limited studies on driving comfort of psychological impact of landscapes. Therefore, constantly changing landscapes under different light conditions should be classified to estimate impacts of resulting classification on driver visual performance. In order to identify impact of the scenes through windshield on driver concentration, different types of landscapes should also be examined. These visual conditions can be exemplified as light of the sun on the road, watching vehicles in crowded traffic, and driving on dark road.

Proposed Approach

In this study, 40 pictures taken within a car have been examined, which are specified as 10 fr, 10 mrht, 10 drht, and 10 rsfs. The pictures taken through the windshield include some inner part of the car that is not related to whole the scene. Therefore, this portion of the image is removed using a filter. Then Linear discriminant analysis algorithm is utilized to select some of effective features (C. Ding and H.C. Peng. 2003). I have developed pie charts to sketch minimum and maximum values of selected features. Analyzing the pie charts I have found that probabilistic distribution of features fits an exponential kernel. By substituting correspondent probabilistic values in to an object function, scenes are classified. Using the resulting values of this classification, the concentration of driver on road is probabilistically investigated. In this way, a state of the art model is proposed to estimate driver concentration using respective scenes that driver look through windshield.

Related Work

In one study using spatial vibrotactile clues of landscapes, visual attention of drivers was investigated to get potential emergency response rate (Shankar, Venkataraman, Fred Mannering, and Woodrow Barfield, 1995). In another paper, authors worked on risk factors for traffic accidents with single vehicle in Hong Kong (Treat, John R, 1979). In this article, the effect of district, human, vehicle, safety, and environmental factors are examined (Ho, Cristy, Hong Z. Tan, and Charles Spence, 2005). As to another study, risk of injury of child bruises was strongly associated with traffic volume risk (Yau, Kelvin KW, 2004).. Injuries at region with highest traffic volumes were 14 times greater than less intensity region (Teran-Santos, J., A, 1999). In some of articles, reasons that cause accidents by diverting the attention of the drivers were investigated (Violanti, John M., and James R. Marshall, 1996). In these works, some of the reasons such as Sleep Apnea, Alzheimer disease, and using a cell phone increase the rate of traffic accidents by distracting drivers (Dubinsky, Richard M., Anthony C. Stein, and Kelly Lyons, 2000). In another paper, nearly half of truck drivers expressed a negative view about technological precautions for driver drowsiness (Ansari, S, 2000).

Contribution

The factors effecting on traffic accidents have been investigated in most of the recent studies. However there are a few researches that are focusing effects of environmental landscape on driver. In this way, performing a risk analysis I are seeking how to affect windshield landscape on performance of driver. In this study Linear discriminant analysis based feature reduction method is exploited. Then Jensen Shannon and Hellinger Distance with exponential kernel are utilized to get object function. Additionally, classifications are probabilistically visualized on a pie chart.

Outline of the Paper

Theories and infrastructure information of the study are given in Section II. Experimental results are explained in Section III. Finally the results obtained are discussed in Section IV.

Materials and Methods

There are many visual factors that influence on driver concentration such as monotonous free road (fr), road scene under frontal full sunlight (rsfs), dark road with heavy traffic (drht), and monotonous road with heavy traffic (mrht). For example, sunlight bothering driver's eyes can impair driving comfort and safety. In this study, under stochastic driving conditions, driver concentration effect for changing landscape has been modeled, and introduced a state of the art approach. Hence, investigating pictures with 10 fr, 10 mrht, 10 drht, and 10 rsfs are taken inside a vehicle.

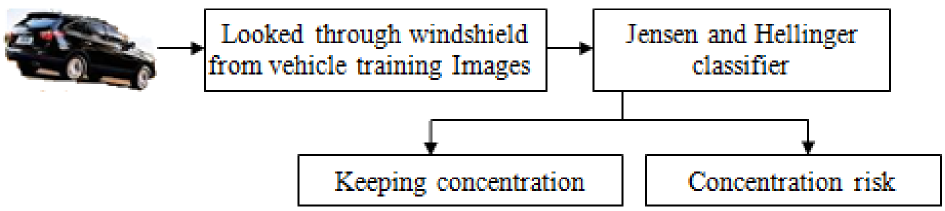

Figure 1. Proposed system

These 40 pictures are preferred as training pictures. The proposed system is shown in Figure 1.
Steps to be followed for the proposed system are

Step 1: 40 pictures are acquired through the windshield. In the pictures, some inner part of the car that is not related to whole the scene is removed using a filter.
Step 2: 10 of them are selected using Linear discriminant analysis.
Step 3: Pie charts are obtained considering minimum and maximum ranges of selected features for pictures with 10fr, 10mrht, 10drht, and 10rsfs as seen in Figure 2. These pie chart limit values are subjected to 3 stages for each feature separately as depicted in Figure 2.

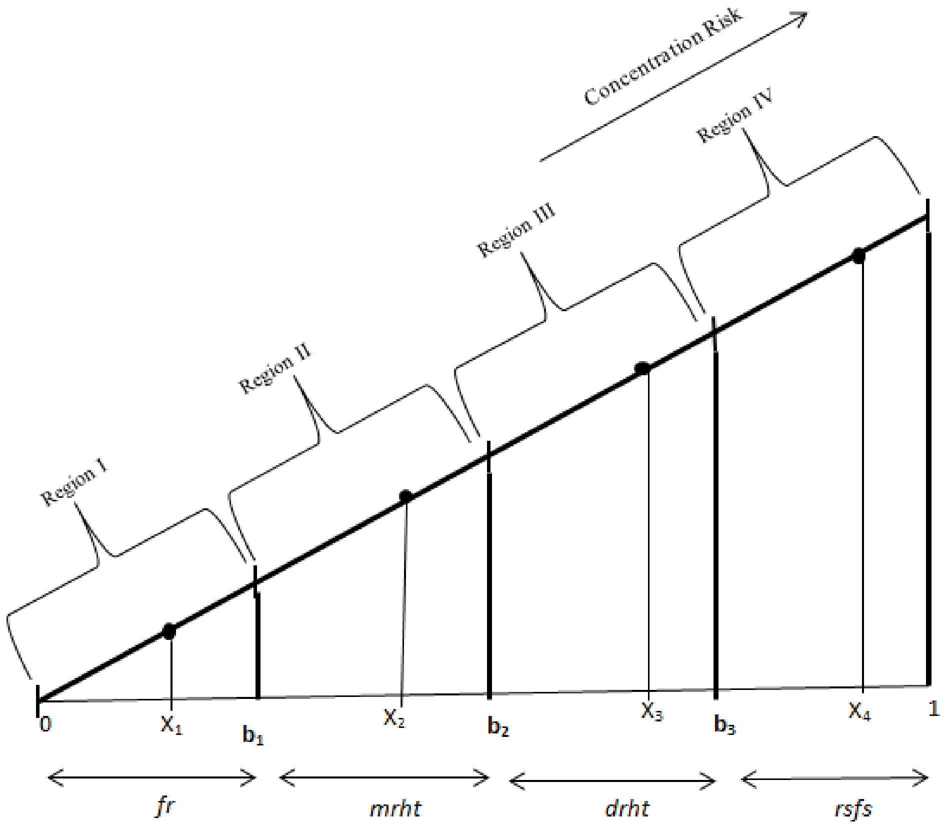

Figure 2. Dial limit values of features in the fr, mrht, drht and rsfs pictures

In Fig. 2, $ffr_i = \{ffr_1, ffr_2, \ldots, ffr_{10}\}$ is feature *i* values of image for *fr*. $frsfs_i = \{frsfs_1, frsfs_2., frsfs_{10}\}$ is feature i values of image for *rsfs*. $fmrht_i = \{fmrht_1, fmrht_2, \ldots, fmrht_{10}\}$ is feature *i* values of image for *mrht*. $fdrht_i = \{fdrht_1, fdrht_2, , fdrht_{10}\}$ is feature *i* values of image for *drht*. ffr_{min} is the smallest feature values of 10 *frv*. ffr_{max} is the biggest feature values of 10 *frv*. $frsfs_{max}$ is the biggest feature values of 10 *rsfs*. $fmrht_{max}$ is the biggest feature values of 10 *mrht*. $fdrht_{max}$ is the biggest feature values of 10 *drht*. Road (R_j) is 10 *fr*, 10 *mrht*, 10 *drht*, and 10 *rsfs*. In Fig. 2, region I is *fr*, Region II is *mrht*, Region III is *drht*, Region IV is *rsfs* . As Stage II is normalized to Stage III, ranges of features can be expressed as

$$x_i = (fR_j - a).1/frsfs_{max} \qquad b_i = (fR_{jmax} - a).1/frsfs_{max} \tag{1}$$

where b_i is the status of maximum feature value normalized to 1, which is obtained from 40 training pictures *fr*, *mrht*, *drht,* and *rsfs*; x_i refers to feature values obtained from pictures. As pie chart values are examined, it is seen that x_i and b_i values are in compliance with exponential distribution. Accordingly, exponential kernel is obtained by

$$P(c|a_{ij}) = 100b_i^{x_i} \tag{2}$$

where $P(c|a_{ij})$ is probabilistic value of the images, *fr, mrht, drht* and *rsfs*.
Step 4: In Stage II, minimum value of *fr* images is subtracted from each of limit rates so that initial value of these values shall be 0. They are normalized in Stage III by means of Eq. (1), and probabilistic ranges are estimated.
Step 5: After training image is normalized to 1, these values indicate exponential distribution rather linear one. This situation can be seen from b_i and x_i rates on the pie chart.
Step 6: Probabilistic values of *fr, mrht, drht* or *rsfs* are found by means of Eq. (2) for exponential kernel.
Step 7: These probabilistic values are used by Eqs. (2) and (3) for each feature associated with concentration rate.

Step 8: The values obtained by Step 7 are substituted by Eqs. (4) and (5) which are weights according to Jensen divergence and Hellinger measure. Therefore weight values for each feature can be found.
Step 9: These weight values are added and multiplied with the value of each feature separately by means of Eq. (6). As a result of this calculation, a probabilistic measure is obtained. The range of this measure is in between 0 and 1 since the rates obtained by Eq. (9) are estimated in a probabilistic way. Thus, closing to 1 means the increase of "Concentration Risk" as seen in Fig. 2, Stage III.

Jensen-Shannon Divergence and Hellinger

Jensen Divergence (Js) and Hellinger (He) measure are given in Eqs. (3) and (4) for 10 *fr*, 10 *mrht*, 10 *drht* and 10 *rsfs* images taken through windshield of vehicle. $P(c|a_{ij})$, in Eq. (2), can be calculated by Bayesian Network probabilistic approach. However, probabilistic distributions of features show conformity with the Exponential Kernel. Initial values of $P(c|a_{ij})$ are obtained from this kernel. $KL(C|a_{ij})$ is the average mutual information between the events c and a_{ij} with the expectation taken with respect to a posteriori probability distribution of (C Lee, Chang-Hwan, Fernando Gutierrez, and Dejing Dou 2011). I can define Kullback- Leibler divergence with naïve Bayesian as

$$KL(C|a_{ij}) = \sum_c P(c|a_{ij})\, log(\frac{P(c|a_{ij})}{P(c)} \tag{3}$$

Progressing Eq. (3) I can find the new measures, which are Jensen Shannon and Hellinger. When Jensen divergence and Hellinger measure in Eq. (4), (5) are put in their place, average weights with respect to Js and He are estimated namely by Eq. (6). Weights calculation Js and He are shown in Eq. (7) as

$$Js(C|a_{ij}) = \sum_c P(c|a_{ij})\, log(\frac{P(c|a_{ij})}{P(c)} \quad + \quad (1 - P(c|a_{ij}))\, log(\frac{(1-P(c|a_{ij}))}{(1-P(c))}) \tag{4}$$

$$He(C|a_{ij}) = \sum_c(\sqrt{P(c|a_{ij})} \quad - \sqrt{(P(c)} \ )^2 \tag{5}$$

$$W_{Jsavg,Heavg}(i) = \sum_{j/i} \frac{(a_{ij})}{N} Js(C|a_{ij}), He(C|a_{ij}) \tag{6}$$

$$W_{Js,He}(i) = \frac{W_{Jsavg,Heavg}(i)}{z\sum_{j/i} P(a_{ij}) \log P(a_{ij})} \tag{7}$$

where $W_{Jsavg,Heavg}(i)$ is average weight calculation of the feature i for Js and He. $W_{Js,He}(i)$ is weight of the feature i for Js and He.

On the other hand, Topsøe (F. Topsøe 2000). mentioned about a close relationship between Hellinger distance and Jensen divergence. Therefore the relationship between Jensen-Shannon and Hellinger can be expressed by

$$\frac{1}{2} He\left(P(c|a_{ij}), (P(c)\right) \leq Js\left(P(c|a_{ij}), (P(c)\right) \leq 2\ln(2)\, He\left(P(c|a_{ij}), (P(c)\right) \tag{8}$$

Decision Making

After calculating weights for each selected feature of images, these weights are put in their places as

$$d_{Jsavg,Heavg} = \frac{argmax \;\; P(c) \prod_{a_{ij} \in d} P(a_{ij}|c)^{W_{Js,He}(i)}}{Si} \tag{9}$$

where a_{ij} is the *j*-th value in *i*-th feature, N is the total number of records, c is the target feature, d_{Js} is test data for Jensen, d_{He} is test data for Hellinger, z is normalization constant, and *Si* is number of sample images for each scene type, that is, *Si*=10 for 10 *fr*, 10 *mrht*, 10 *drht*, and 10 *rsfs*.

$$Concentration \;\; Risk = \frac{d_{Jsavg} + d_{Heavg}}{2} \tag{10}$$

The concentration risk can be estimated using the average of d_{Jsavg} and d_{Heavg} as seen in Eq. (9).

Results and Discussion

Some of samples out of 40 pictures are given in Figure 3.

Figure 3. Sample images through windshield for *fr, mrht, drht, rsfs*

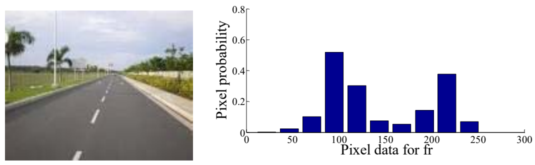

(a) (b)

Figure 4. (a) Image (fr1)(b) Probabilistic distribution of image in (a)

Probabilistic density distributions of the image fr2, in and Figure 4 are shown at right side of same images. All the Equations between (9-10) the values of d_{Js} and d_{He} are obtained in Figure 5.

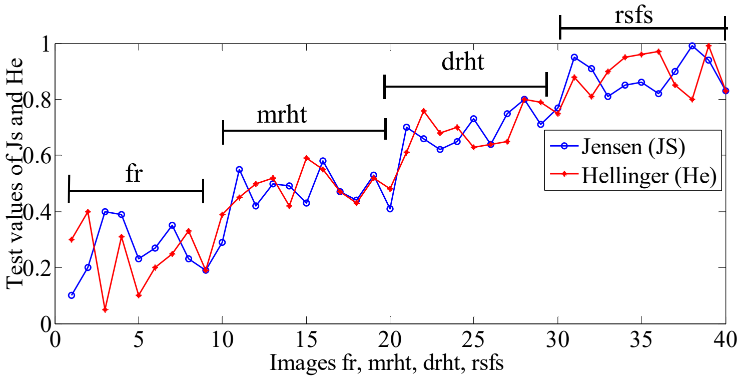

Figure 5. $d_{js,\,dHe}$ values for images fr, mrht, drht and rsfs

Reviewing Figure 5, the $d_{js,he}$ values of fr images are in the range between 0-0.4; the $d_{js,he}$ values of mrht images are in the range between 0.4-0.6; the $d_{js,he}$ values of drht images are in the range between 0.6-0.8, and the $d_{js,he}$ values of rsfs images are in the range between 0.8-1 are found. Table 1 is obtained by Figure 5.

Table 1: D_{Jsort}, D_{Heort} and Concentrarion Risk (*Conr)* Rates of *fr, mrht, drht and rsfs for* 40 İmages

	fr	**mrht**	**drht**	**rsfs**
d_{Jsort}	0.251	0.534	0.701	0.894
d_{Heort}	0.265	0.482	0.703	0.886
$Concentration\ Risk\ (Conr)$	0.258	0.508	0.702	0.89

According to *Conr* row in Table 1, I can conclude that

$$Conr_{fr} < Conr_{mrht} < Conr_{drht} < Conr_{rsfs}$$

It suggests concentration risk rate of *fr* is less than all the other road models. However, concentration risk rate of *rsfs* is more than all the other road models.

Conclusion

In this work, 40 training images taken through windshield of the vehicle are examined. Object function for the images *fr, mrht, drht*, and *rsfs* is obtained by Jensen Shannon Divergence and Bhattacharya Distance. The results are found as concentration risk via proposed decision-making algorithm. Consequently, I estimate the impact of landscape through the windshield on driver concentration. It suggests concentration risk rate of *fr* is less than all the other road models. However, concentration risk rate of *rsfs* is more than all the other road models. As a next step of this study all the frames along the road could be combined. Hence, this information would be a complementary clue for the studies on driver behavior.

References

C. Ding and H.C. Peng.(2003). “Minimum Redundancy Feature Selection from Microarray Gene Expression Data,” Proc. Second IEEE Computational Systems Bioinformatics Conf. pp. 523-528, 2003.

Shankar, Venkataraman, Fred Mannering, and Woodrow Barfield. (1995). "Effect of roadway geometrics and environmental factors on rural freeway accident frequencies," Accident Analysis & Prevention 27.3, 371-389.

Treat, John R.(1979). "Tri-level study of the causes of traffic accidents: final report. Executive summary," 1979.

Ho, Cristy, Hong Z. Tan, and Charles Spence. (2005) "Using spatial vibrotactile cues to direct visual attention in driving scenes." *Transportation Research Part F: Traffic Psychology and Behaviour* 8.6, 397-412, 2005.

Yau, Kelvin KW,(2004)."Risk factors affecting the severity of single vehicle traffic accidents in Hong Kong," *Accident Analysis & Prevention* 36.3, 333-340.

Roberts, I.,(1985). "Effect of environmental factors on risk of injury of child pedestrians by motor vehicles: a case-control study," *Bmj* 310.6972 (1995): 91-94.H. Poor, *An Introduction to Signal Detection and Estimation*. New York: Springer-Verlag.

Teran-Santos, J., A. (1999). Jimenez-Gomez, and J. Cordero-Guevara, "The association between sleep apnea and the risk of traffic accidents," *New England Journal of Medicine* 340.11, 847-851, .

Violanti, John M., and James R. Marshall (1996). "Cellular phones and traffic accidents: an epidemiological approach," *Accident Analysis & Prevention* 28.2, 265-270.

Dubinsky, Richard M., Anthony C. Stein, and Kelly Lyons (2000). "Practice parameter: Risk of driving and Alzheimer’s disease (an evidence-based review) Report of the Quality Standards Subcommittee of the American Academy of Neurology," Neurology 54.12, 2205-2211.

Ansari, S. (2000). "Causes and effects of road traffic accidents in Saudi Arabia," *Public health* 114.1, 37-39.

Lee, Chang-Hwan, Fernando Gutierrez, and Dejing Dou (2011). "Calculating feature weights in naive bayes with Kullback-Leibler measure," Data Mining (ICDM), 2011 IEEE 11th International Conference on. IEEE.

F. Topsøe (2000). Some inequalities for information divergence and related measures of discrimination, IEEE Trans. Information Theory, 44(4):1602–1609.

